Shock-capturing Schemes for a Collisionless Two-fluid Plasma Model

E. Alec Johnson
Department of Mathematics, UW-Madison
Presented on August 29, 2007
at Sandia National Laboratories

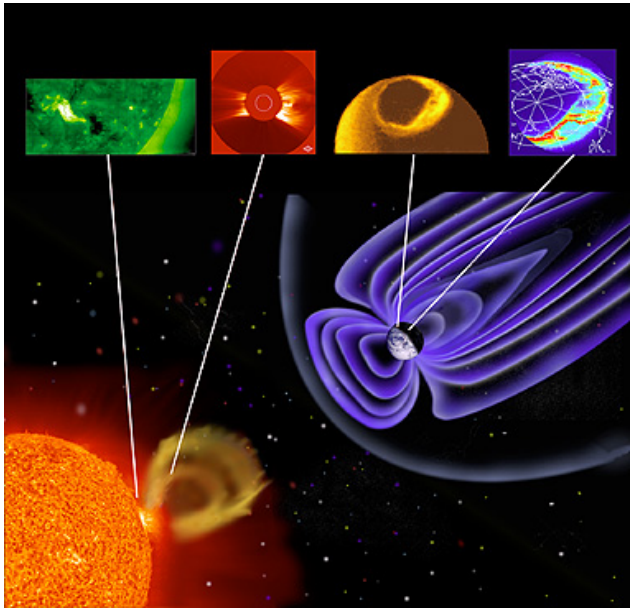

©2003, Kenneth Lang, Tufts University

Motivation: magnetic reconnection

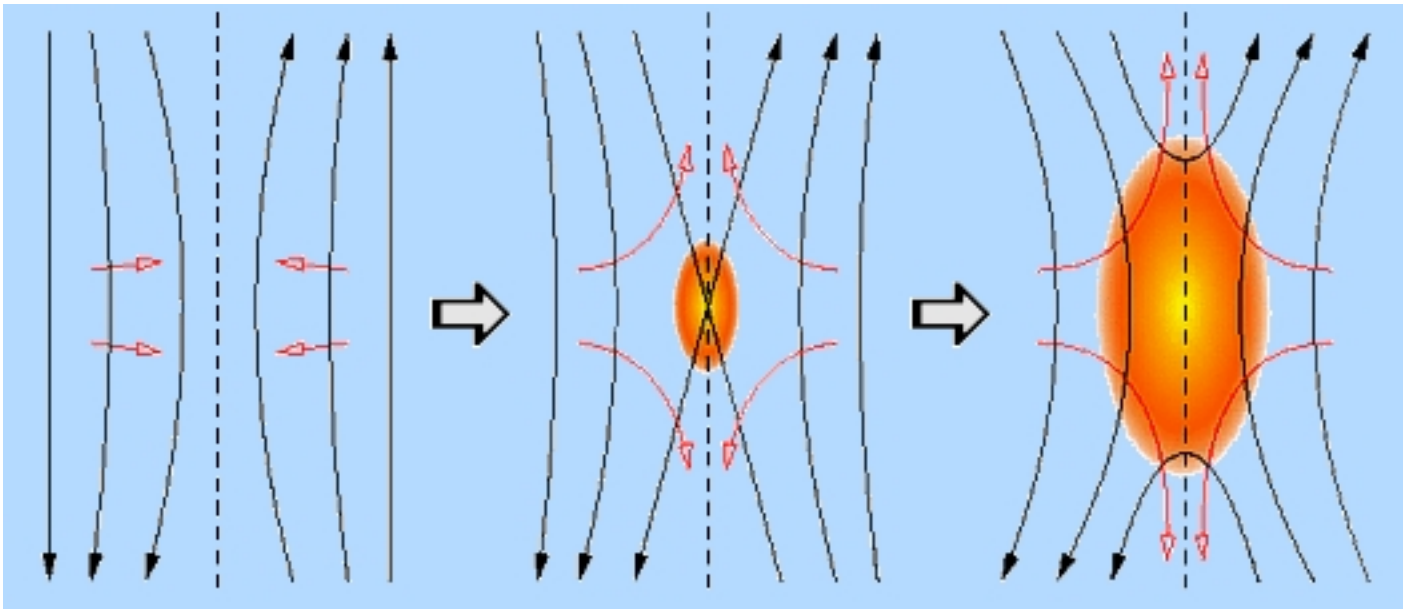

http://www.aldebaran.cz/astrofyzika/plazma/reconnection_en.html

Calculations: Brio-Wu shock problem

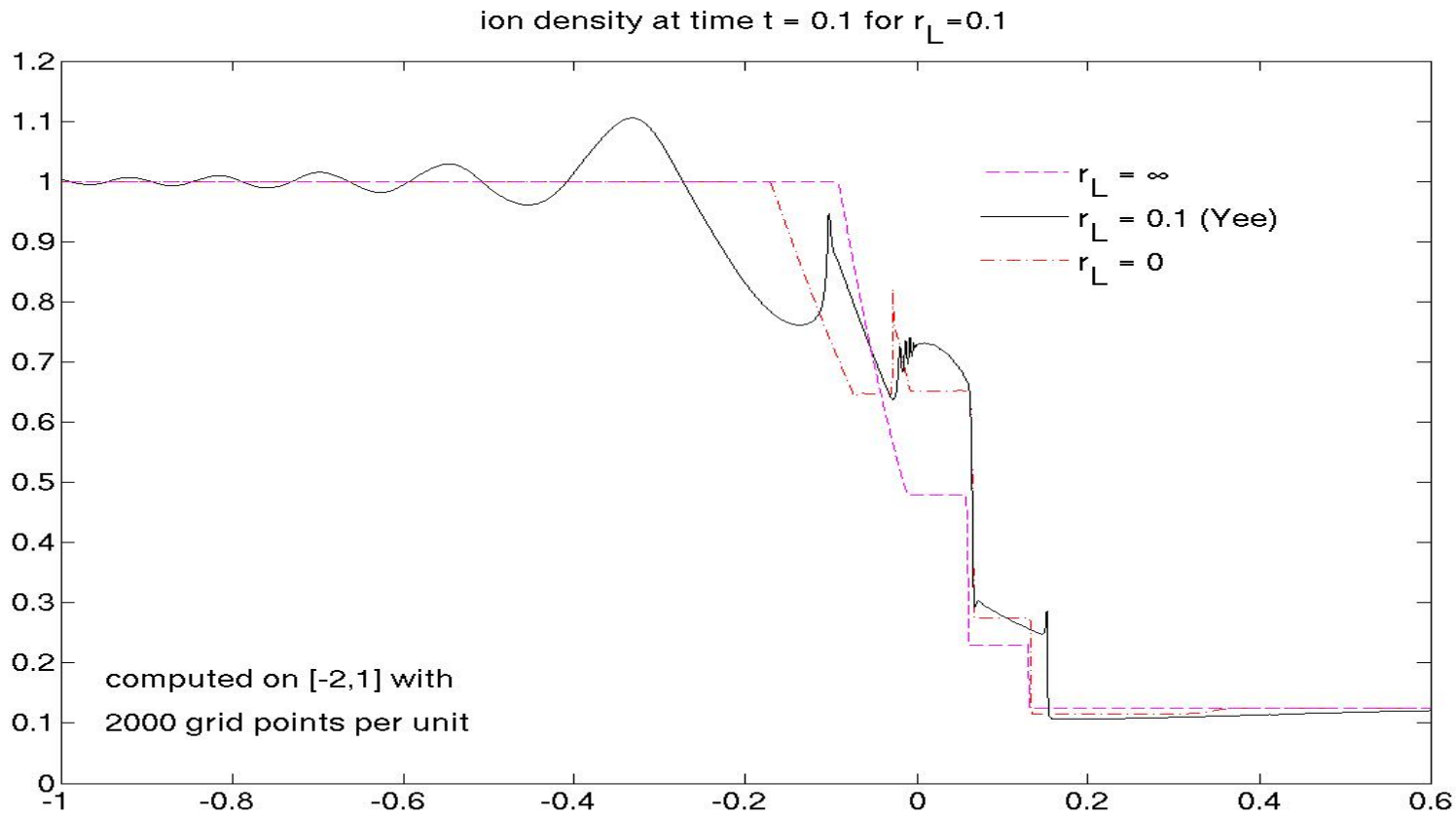

Outline

1. Problem: space weather and fast reconnection
2. Physical model: two-fluid plasma
3. Computations: Brio-Wu 1D shock problem
4. Ideas for future work

Problem: Space weather

Broad goal: to model **space weather**.

- Earth bombarded with **solar wind**.
  1. *charged*: mostly protons or electrons.
  2. *sparse*: 5-10 protons (or electrons) per cm^3.
  3. *fast-moving*: proton velocities of 200–800 km/s (.1%–.3% light speed).
- Solar wind varies dramatically.
- Solar storms cause **geomagnetic storms**.

Problem: Space weather

How does the solar wind interact with Earth's magnetic field?

- Solar wind is decelerated at the bow shock.
- Solar wind is generally deflected around the magnetopause.
- But reconnection of magnetic field lines allows plasma to cross the magnetopause into Earth's magnetosphere.

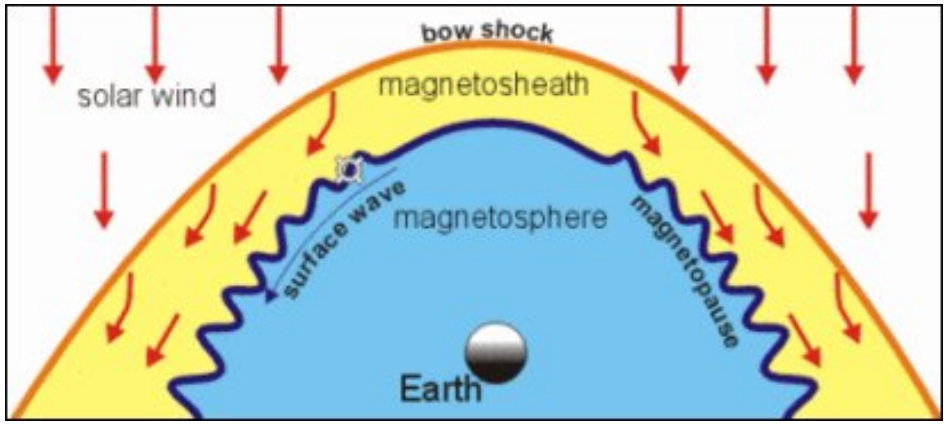

(cross-section along ecliptic)

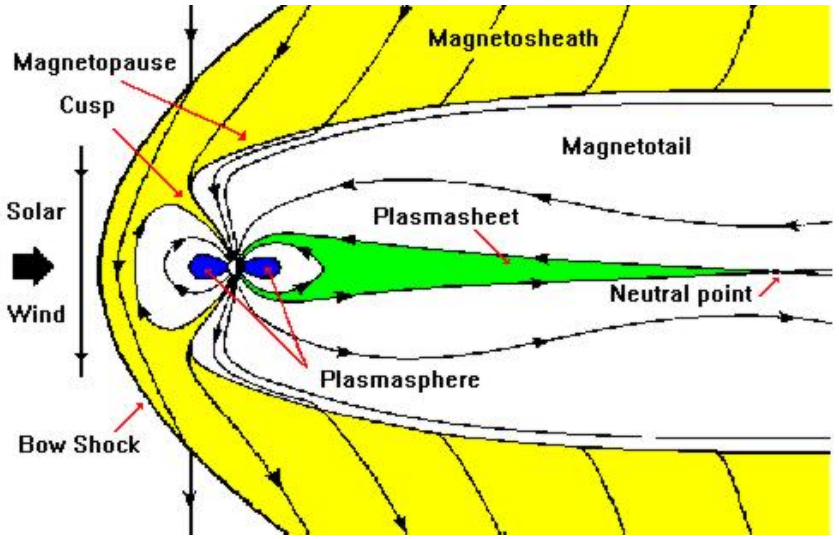

(cross-section along polar axis)

Problem: Space weather: Magnetosphere

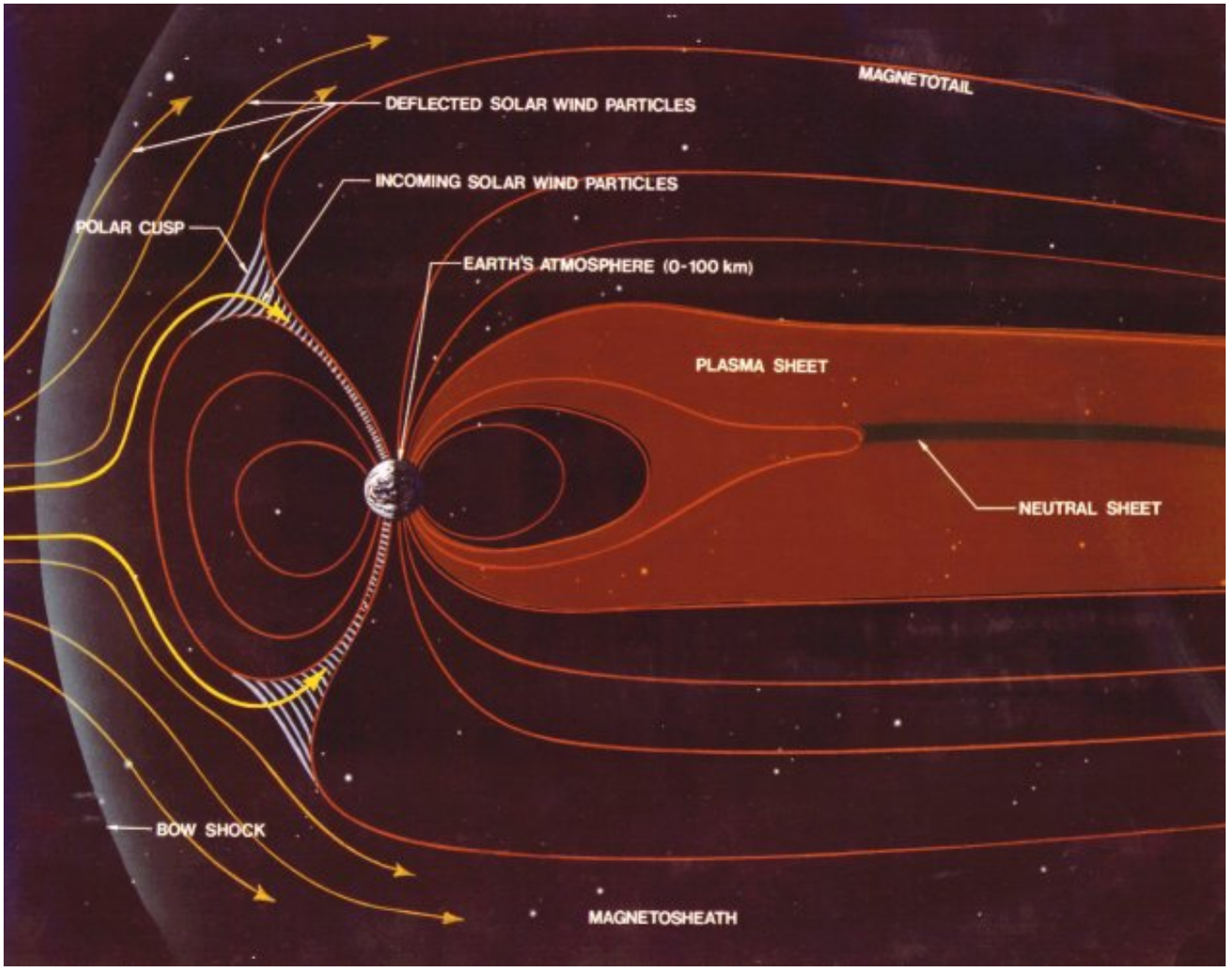

Problem: Space weather: Magnetosphere

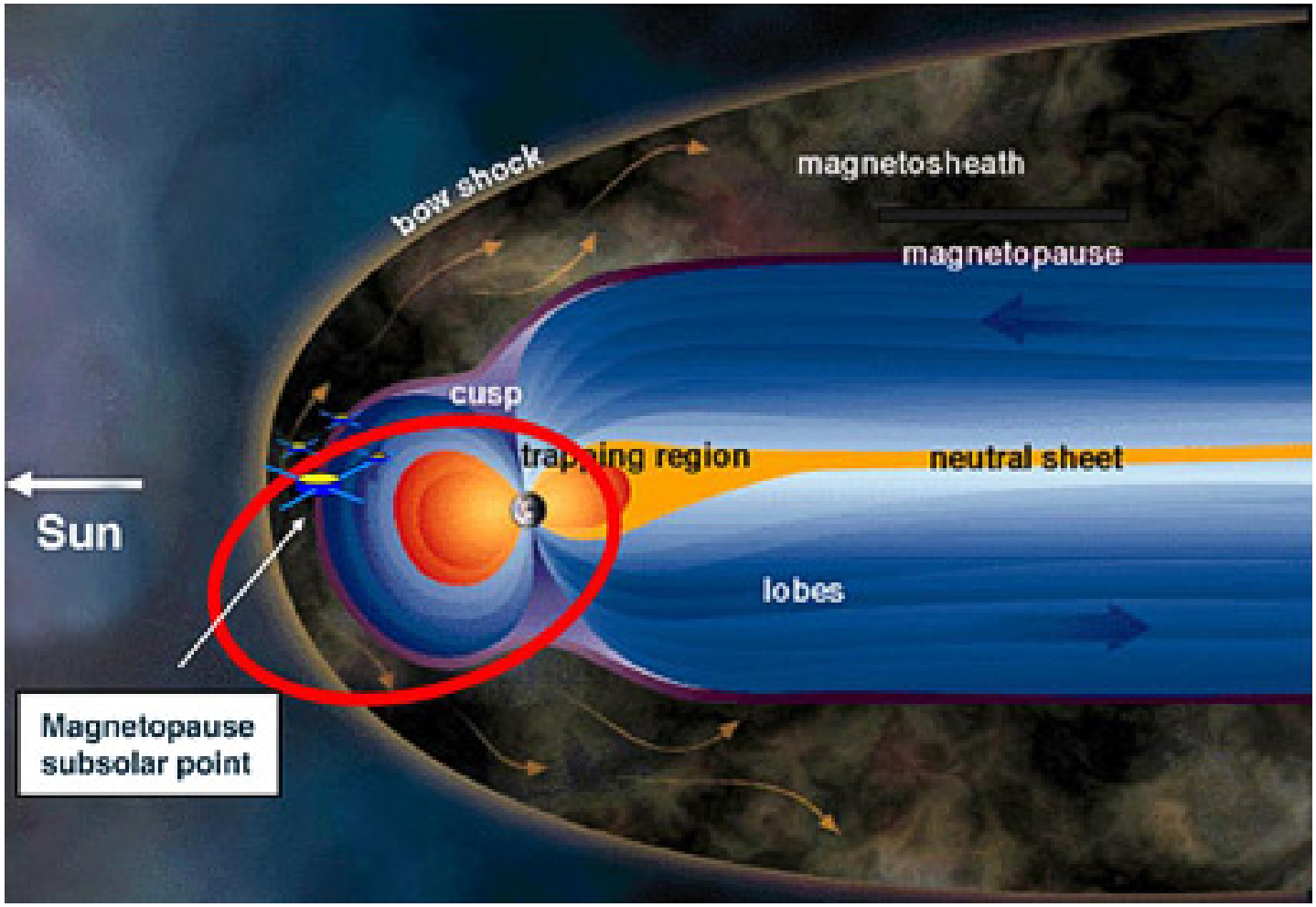

The red circle indicates the position of the four satellites of the European Space Agency's Cluster fleet.

Credits: ESA

Problem: Magnetic reconnection

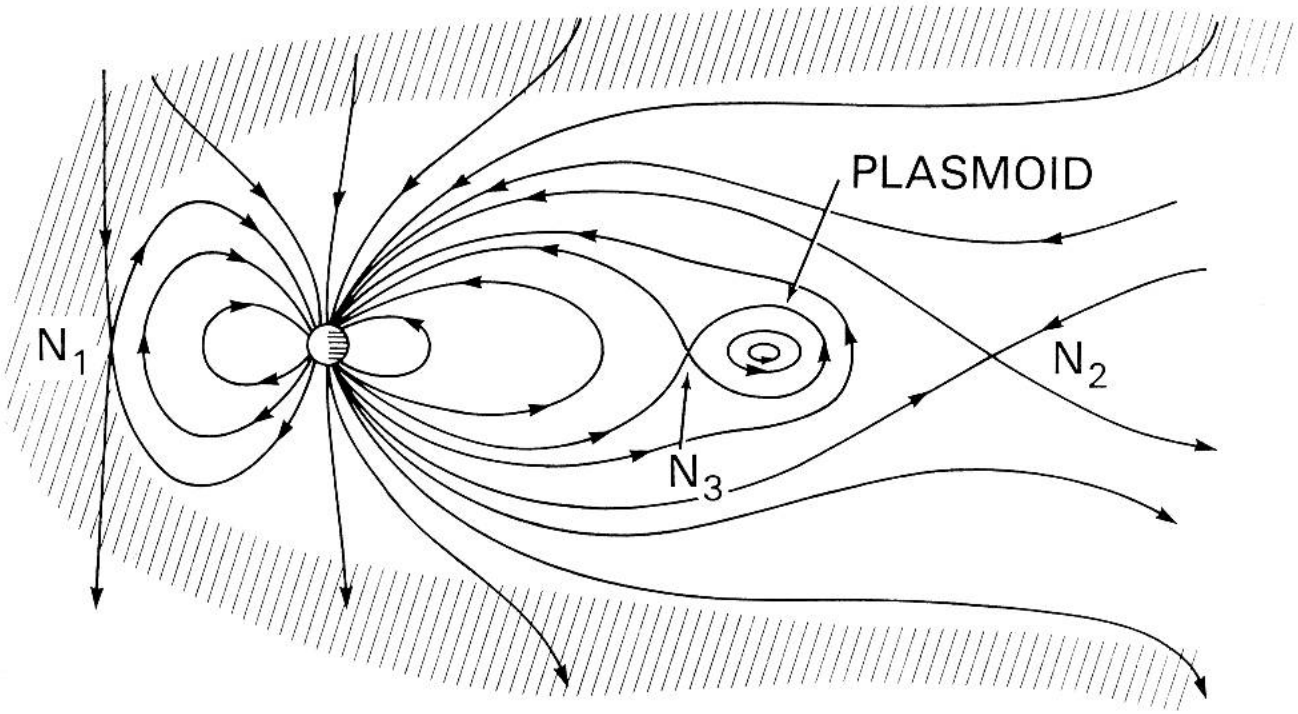

Reconnection at dayside and magnetotail.

Problem: Magnetic reconnection

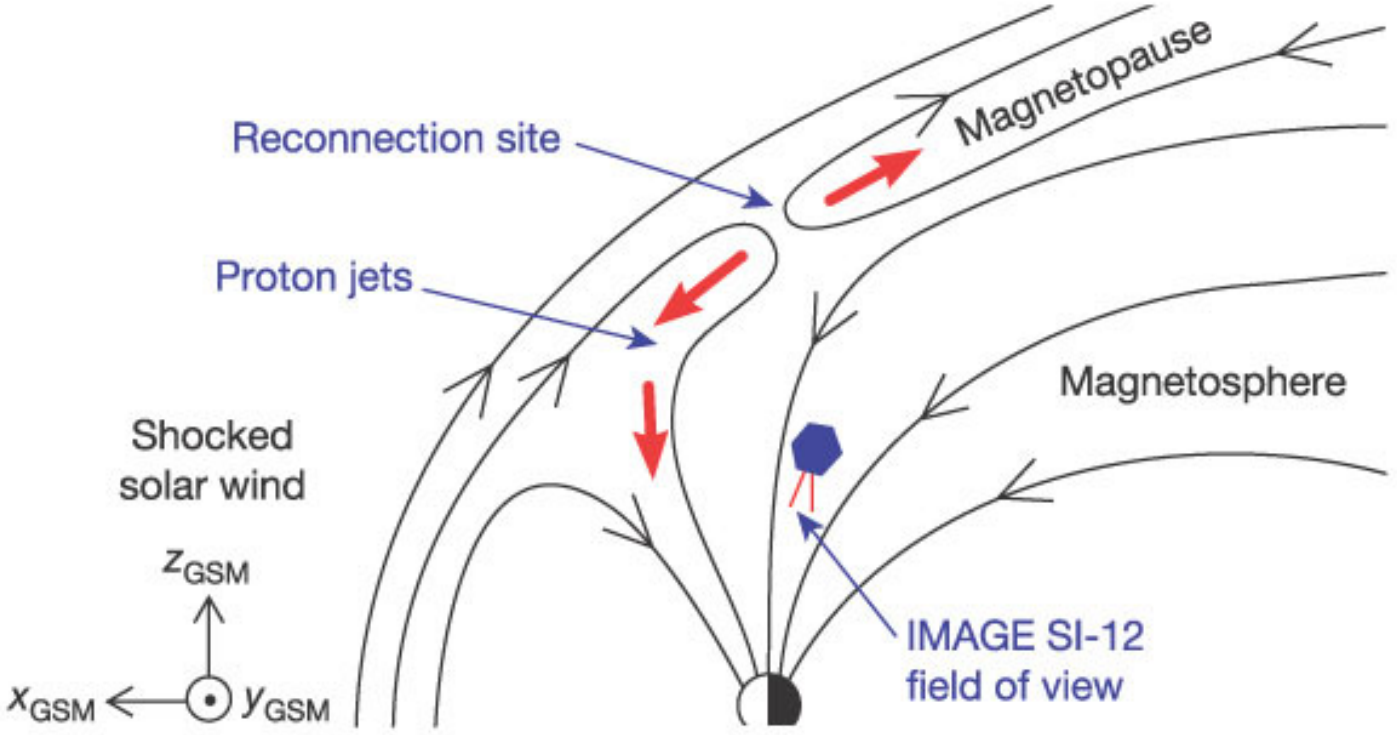

Solar wind reconnecting at magnetopause

From *Continuous magnetic reconnection at Earth's magnetopause*,
H. U. Frey, T. D. Phan, S. A. Fuselier and S. B. Mende,

Nature 426, 533-537(4 December 2003)

Problem: Magnetic reconnection

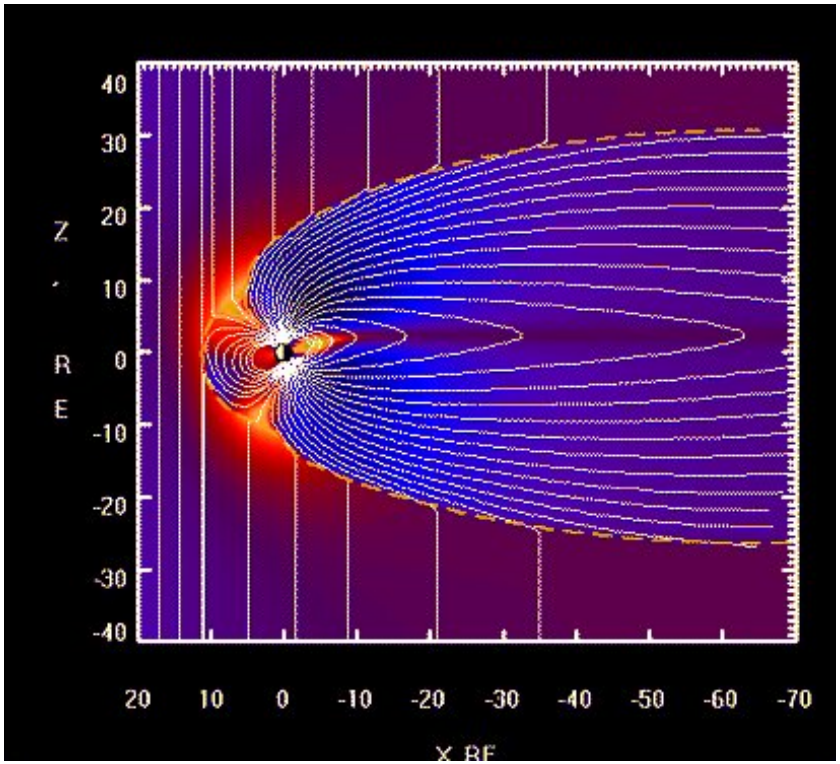

Solar wind reconnecting at magnetopause

14-Aug-2007 21:03:37 UT
Schematic of Reconnection
Date: 03 Feb 2005
Satellite: Cluster
Depicts: Reconnecting field lines

Copyright: N. Tsyganenko, USRA/GSFC/NASA

Problem: Fast magnetic reconnection

Our project is to develop an efficient algorithm that (1) *captures shocks* and (2) resolves **fast magnetic reconnection**.

(1) Solar wind produces strong shocks.

(2) Fast magnetic reconnection is critical to modeling space weather events.
   (a) Fast reconnection seems to make violent solar storms possible.
   (b) Reconnection is the primary mechanism that allows gusts of solar wind to penetrate the magnetosphere and generate geomagnetic storms.

Problem: Fast solver

How can we make our algorithm efficient?

- Solvers that resolve fast reconnection (and by implication fast waves) tend to be computationally expensive due to the need for a short time step.
- Reconnection is generally restricted to specific regions of space, and elsewhere cheaper models that don't resolve fast waves are accurate enough.
- Our strategy: **Can we selectively resolve fast waves in regions where magnetic reconnection is occurring, and elsewhere use a coarser time step?**

Physical model: Criteria

Criteria to choose a model:

① The model should admit the phenomena of interest (e.g., *fast reconnection*).

② The model should allow an algorithm that is *fast* and preferable *simple*.

Physical model: Available models

Hierarchy of available models:

① **Kinetic models**.
  (a) **Fully kinetic models**. (particle density function $f_s(\mathbf{x}, \mathbf{v}, t)$ for both species s.)
    - Most accurate but too expensive.
  (b) **Hybrid models**. (an electrons fluid and kinetic ions.)
    - Gets reconnection width correct.

② **Two-fluid models.** (an electron fluid and an ion fluid.)
  (a) **Collisionless ideal two-fluid model.** (ideal gas for each fluid, fluids coupled only to electromagnetic field, not directly to one another.)
    - Admits fast reconnection.
    - fastest wave: light wave.

③ **One-fluid** models.
  (quasineutral conducting fluid.)
  (a) **Hall MHD**. (Ohm's law with Hall term.)
    - Admits fast reconnection.
    - Fastest wave: whistler wave at numerically controlled speed.
  (b) **MHD**. (Simplified Ohm's law.)
    - (**Resistive MHD** converges to the correct steady state, but too slowly by orders of magnitude; **ideal MHD** does not admit reconnection.)
    - Fastest wave: fast magnetosonic wave

Physical model: Our choice of plasma model

- We have focused on the **collisionless two-fluid model** rather than Hall MHD.
  - The simplicity of the two-fluid model lends itself to explicit shock-capturing methods.
    - Hall MHD has a differentiated source term, whereas collisionless two-fluid has an undifferentiated source term.
- We compare our computations with ideal MHD, which should be sufficiently accurate in the majority of the domain where reconnection is absent.

Model equations: Conservation law framework

Since we are developing shock-capturing methods, we express our equations as conservation or balance laws.

$$\underline{q}_t + \underline{\nabla} \cdot \underline{\underline{f}}(\underline{q}) = \underline{s}(\underline{q}).$$

- $\underline{q}$ is the state (mass, momentum, energy, and electromagnetic field),
- $\underline{\underline{f}}$ is the flux, and
- $\underline{s}$ is the source term.

Model equations: Two-fluid model

The two-fluid model consists of gas dynamics for each of the two fluids, coupled to Maxwell's equations by means of source terms consisting of the Lorentz force, the charge density, and the current and displacement currents. The gas dynamics equations are

$$\partial_t \underbrace{\begin{bmatrix} \rho_s \\ \rho_s \mathbf{v}_s \\ \mathcal{E}_s \end{bmatrix}}_{\text{conserved}} + \nabla \cdot \underbrace{\begin{bmatrix} \rho_s \mathbf{v}_s \\ \rho_s \mathbf{v}_s \mathbf{v}_s + p_s \mathbb{I} \\ \mathbf{v}_s \left(\mathcal{E}_s + p_s \right) \end{bmatrix}}_{\text{hyperbolic flux}} = \underbrace{\begin{bmatrix} 0 \\ \frac{q_s}{m_s} \rho_s (\mathbf{E} + \mathbf{v}_s \times \mathbf{B}) \\ \frac{q_s}{m_s} \rho_s \mathbf{v}_s \cdot \mathbf{E} \end{bmatrix}}_{\text{electromagnetic source}},$$

where $s = i$ (ion) or e (electron), $\frac{q_s}{m_s}$ is charge-to-mass ratio, ρ is mass density, $\mathbf{v}$ is fluid velocity, $\mathcal{E}$ is energy, p is pressure, and $\mathbf{E}$ and $\mathbf{B}$ are electric and magnetic field, We assume the ideal gas constitutive relations $\mathcal{E}_s = \frac{p_s}{\gamma_s - 1} + \frac{1}{2} \rho_s v_s^2$. The charge density and the current density of each species are given by the relations $\sigma_s = \frac{q_s}{m_s} \rho_s$ and $\mathbf{J}_s = \frac{q_s}{m_s} \rho_s \mathbf{v}_s$.

Maxwell's equations for the evolution of the electromagnetic field are

$$\underbrace{\partial_t \begin{bmatrix} c\mathbf{B} \\ \mathbf{E} \end{bmatrix} + c\nabla \times \begin{bmatrix} \mathbf{E} \\ -c\mathbf{B} \end{bmatrix} = \begin{bmatrix} 0 \\ -\mathbf{J}/\epsilon_0 \end{bmatrix}}_{\text{evolution equations}} \text{ and } \underbrace{\nabla \cdot \begin{bmatrix} c\mathbf{B} \\ \mathbf{E} \end{bmatrix} = \begin{bmatrix} 0 \\ \sigma/\epsilon_0 \end{bmatrix}}_{\text{constraint equations}},$$

where $\mathbf{B}$ = magnetic field, $\mathbf{E}$ = electric field, $\sigma = \sigma_i + \sigma_e$ = net charge density, $\mathbf{J} = \mathbf{J}_i + \mathbf{J}_e$ = net current, c = light speed, and ϵ_0 = permittivity of free space.

Model equations: Nondimensionalization

We nondimensionalized to minimize the number of parameters in the two-fluid system.

Chosen characteristic values.

$x_0 =$ typical length scale

$v_0 =$ typical thermal velocity of an ion

$n_0 =$ typical number density

$B_0 =$ typical magnetic field strength

$m_0 =$ mass of an ion

$q_0 =$ charge strength of ion/electron

Immediate nondimensionalizations.

$$\mathbf{v}_s = v_0 \widehat{\mathbf{v}}_s$$

$$n_s = n_0 \widehat{n}_s$$

$$\mathbf{B} = B_0 \widehat{\mathbf{B}}$$

Implied nondimensionalizations.

$$t = t_0 \widehat{t} \quad \text{where} \quad t_0 := \frac{x_0}{v_0}$$

$$\partial_t = \frac{1}{t_0} \partial_{\widehat{t}}$$

$$\nabla = \frac{1}{x_0} \widehat{\nabla} \quad \text{where} \quad \widehat{\nabla} := \nabla_{\widehat{\mathbf{x}}}$$

$$m_s = m_0 \widehat{m}_s \quad \text{where} \quad m_0 := m_i$$

$$\text{and} \quad \widehat{m}_s = \begin{cases} 1 & \text{if } s = i \\ \frac{m_e}{m_i} & \text{if } s = e \end{cases}$$

$$q_s = q_0 \widehat{q}_s \quad \text{where} \quad q_0 := e$$

$$\text{and} \quad \widehat{q}_s = \begin{cases} 1 & \text{if } s = i \\ -1 & \text{if } s = e \end{cases}$$

$$\rho_s = \rho_0 \widehat{\rho}_s \quad \text{where} \quad \rho_0 := m_0 n_0$$

$$\sigma_s = \sigma_0 \widehat{\sigma}_s \quad \text{where} \quad \sigma_0 := q_0 n_0$$

$$\mathbf{J}_s = J_0 \widehat{\mathbf{J}}_s \quad \text{where} \quad J_0 := q_0 n_0 v_0$$

$$p_s = p_0 \widehat{p}_s \quad \text{where} \quad p_0 := \rho_0 v_0^2 = m_0 n_0 v_0^2$$

$$\mathcal{E}_s = \mathcal{E}_0 \widehat{\mathcal{E}}_s \quad \text{where} \quad \mathcal{E}_0 := p_0$$

$$\mathbf{E} = E_0 \widehat{\mathbf{E}} \quad \text{where} \quad E_0 := B_0 v_0$$

Relations:

$$\widehat{\mathbf{J}}_i = \widehat{\rho}_i \widehat{\mathbf{v}}_i, \qquad \widehat{\sigma}_i = \widehat{n}_i = \widehat{\rho}_i,$$
$$-\widehat{\mathbf{J}}_e = \frac{m_i}{m_e} \widehat{\rho}_e \widehat{\mathbf{v}}_e, \qquad -\widehat{\sigma}_e = \widehat{n}_e = \frac{m_i}{m_e} \widehat{\rho}_e.$$

Model equations: Nondimensionalized two-fluid model

Our nondimensionalized equations:

$$\partial_{\widehat{t}} \begin{bmatrix} \widehat{\rho}_i \\ \widehat{\rho}_e \\ \widehat{\rho}_i \widehat{\mathbf{v}}_i \\ \widehat{\rho}_e \widehat{\mathbf{v}}_e \\ \widehat{\mathcal{E}}_i \\ \widehat{\mathcal{E}}_e \end{bmatrix} + \widehat{\nabla} \cdot \begin{bmatrix} \widehat{\rho}_i \widehat{\mathbf{v}}_i \\ \widehat{\rho}_e \widehat{\mathbf{v}}_e \\ \widehat{\rho}_i \widehat{\mathbf{v}}_i \widehat{\mathbf{v}}_i + \widehat{p}_i \, \mathbb{I} \\ \widehat{\rho}_e \widehat{\mathbf{v}}_e \widehat{\mathbf{v}}_e + \widehat{p}_e \, \mathbb{I} \\ \widehat{\mathbf{v}}_i \left(\widehat{\mathcal{E}}_i + \widehat{p}_i \right) \\ \widehat{\mathbf{v}}_e \left(\widehat{\mathcal{E}}_e + \widehat{p}_e \right) \end{bmatrix} = \frac{1}{\widehat{r_L}} \begin{bmatrix} 0 \\ 0 \\ \widehat{\rho}_i (\widehat{\mathbf{E}} + \widehat{\mathbf{v}}_i \times \widehat{\mathbf{B}}) \\ -\frac{m_i}{m_e} \widehat{\rho}_e (\widehat{\mathbf{E}} + \widehat{\mathbf{v}}_e \times \widehat{\mathbf{B}}) \\ \widehat{\rho}_i \widehat{\mathbf{v}}_i \cdot \widehat{\mathbf{E}} \\ -\frac{m_i}{m_e} \widehat{\rho}_e \widehat{\mathbf{v}}_e \cdot \widehat{\mathbf{E}} \end{bmatrix},$$

$$\partial_{\widehat{t}} \begin{bmatrix} \widehat{c}\widehat{\mathbf{B}} \\ \widehat{\mathbf{E}} \end{bmatrix} + \widehat{c\nabla\times} \begin{bmatrix} \widehat{\mathbf{E}} \\ -\widehat{c}\widehat{\mathbf{B}} \end{bmatrix} = \begin{bmatrix} 0 \\ -\widehat{\mathbf{J}}/\epsilon \end{bmatrix}, \text{ and } \widehat{\nabla} \cdot \begin{bmatrix} \widehat{c}\widehat{\mathbf{B}} \\ \widehat{\mathbf{E}} \end{bmatrix} = \begin{bmatrix} 0 \\ \widehat{\sigma}/\epsilon \end{bmatrix}.$$

- $r_L := \frac{m_0 v_0}{q_0 B_0}$ is the **Larmor radius**, the radius of curvature of the circular motion of a typical ion moving perpendicular to a characteristic magnetic field ($\widehat{r_L} := r_L / x_0$),
- $\epsilon := \frac{1}{\widehat{r_L} \widehat{\lambda_D}^2}$ plays the role of permittivity, and
- $\widehat{\lambda_D}$ is the ratio of the Debye length to the Larmor radius. The **Debye length**, $\sqrt{\frac{\epsilon_0 m_0 v_0^2}{n_0 q_0^2}}$, is the distance scale over which electrons screen out electric fields in plasmas (i.e. the distance scale over which significant charge separation can occur). n_0 is a typical value for number density.

Model equations: Ideal MHD

If we consider an asymptotic limit of the two-fluid equations as the Larmor radius r_L goes to zero, we obtain (some of?) the following assumptions used in deriving the MHD equations:

① $\sigma \approx 0$ (quasineutrality)

② $\partial_t \mathbf{E} \approx 0$ (Ampere's law)

③ $\mathbf{E} \approx \mathbf{B} \times \mathbf{v}$ (Ohm's law)

④ $E^2 \approx 0$ (small $\mathbf{E}$)

The work we report compares the two-fluid plasma model with ideal MHD as we take the Larmor radius r_L to zero. The full system of ideal MHD equations is

$$\frac{\partial}{\partial t}\begin{bmatrix}\rho\\ \rho\mathbf{v}\\ \tilde{\mathcal{E}}\\ \mathbf{B}\end{bmatrix} + \nabla\cdot\underbrace{\begin{bmatrix}\rho\mathbf{v}\\ \rho\mathbf{v}\mathbf{v} + \tilde{p}\,\mathbb{I} - \frac{1}{\mu_0}\mathbf{B}\mathbf{B}\\ \mathbf{v}\left(\tilde{\mathcal{E}} + \tilde{p}\right) - \frac{1}{\mu_0}\mathbf{B}\mathbf{B}\cdot\mathbf{v}\\ \mathbf{v}\mathbf{B} - \mathbf{B}\mathbf{v}\end{bmatrix}}_{\text{hyperbolic flux}} = 0$$

and the physical constraint $\nabla \cdot \mathbf{B} = 0$, where ρ is the mass density, $\mathbf{v}$ is the fluid velocity field, $\tilde{\mathcal{E}} := \mathcal{E} + \frac{1}{2\mu_0}B^2$ is the total energy (gas-dynamic energy plus magnetic energy), $\mathbf{B}$ is the magnetic field, and $\tilde{p} := p + \frac{1}{2\mu_0}B^2$ is the total pressure (gas-dynamic pressure plus magnetic pressure). The gas-dynamic pressure is $p = (\gamma - 1)(\mathcal{E} - \frac{1}{2}\rho v^2)$, where $\gamma = \frac{5}{3}$ is the ratio of specific heats.

Numerical method: Operator splitting

Shock-capturing limits us to first-order accuracy in shock-influenced regions. We aim for second-order accuracy for smooth data. This justifies operator splitting:

① ODE solver

② Hyperbolic PDE solver

(a) Gas-dynamics solver (explicit, shock-capturing)

(b) Maxwell solver (ultimately implicit)

Numerical method: ODE solver

We used RK4 to solve the ODE:

$$\partial_{\widehat{t}} \begin{bmatrix} \widehat{\rho}_i \\ \widehat{\rho}_e \\ \widehat{\rho}_i \widehat{\mathbf{v}}_i \\ \widehat{\rho}_e \widehat{\mathbf{v}}_e \\ \widehat{\mathcal{E}}_i \\ \widehat{\mathcal{E}}_e \\ \widehat{\mathbf{B}} \\ \widehat{\mathbf{E}} \end{bmatrix} = \frac{1}{\widehat{r_L}} \begin{bmatrix} 0 \\ 0 \\ \widehat{\rho}_i \widehat{\mathbf{E}} + \widehat{\rho}_i \widehat{\mathbf{v}}_i \times \widehat{\mathbf{B}} \\ -\frac{m_i}{m_e}(\widehat{\rho}_e \widehat{\mathbf{E}} + \widehat{\rho}_e \widehat{\mathbf{v}}_e \times \widehat{\mathbf{B}}) \\ \widehat{\rho}_i \widehat{\mathbf{v}}_i \cdot \widehat{\mathbf{E}} \\ -\frac{m_i}{m_e} \widehat{\rho}_e \widehat{\mathbf{v}}_e \cdot \widehat{\mathbf{E}} \\ 0 \\ \frac{-1}{\widehat{\lambda_D}^2} \left(\widehat{\rho}_i \widehat{\mathbf{v}}_i - \frac{m_i}{m_e} \widehat{\rho}_e \mathbf{v}_e \right) \end{bmatrix}$$

Numerical method: Hyperbolic PDE solver

The hyperbolic part decouples into three independent systems:

① Gas-dynamics for ions

$$\partial_{\widehat{t}} \begin{bmatrix} \widehat{\rho}_i \\ \widehat{\rho}_i \widehat{\mathbf{v}}_i \\ \widehat{\mathcal{E}}_i \end{bmatrix} + \widehat{\nabla \cdot} \begin{bmatrix} \widehat{\rho}_i \widehat{\mathbf{v}}_i \\ (\widehat{\rho}_i \widehat{\mathbf{v}}_i) \widehat{\mathbf{v}}_i + \widehat{p}_i \, \mathbb{I} \\ \widehat{\mathbf{v}}_i \left(\widehat{\mathcal{E}}_i + \widehat{p}_i \right) \end{bmatrix} = 0$$

② Gas-dynamics for electrons

$$\partial_{\widehat{t}} \begin{bmatrix} \widehat{\rho}_e \\ \widehat{\rho}_e \widehat{\mathbf{v}}_e \\ \widehat{\mathcal{E}}_e \end{bmatrix} + \widehat{\nabla \cdot} \begin{bmatrix} \widehat{\rho}_e \widehat{\mathbf{v}}_e \\ (\widehat{\rho}_e \widehat{\mathbf{v}}_e) \widehat{\mathbf{v}}_e + \widehat{p}_e \, \mathbb{I} \\ \widehat{\mathbf{v}}_e \left(\widehat{\mathcal{E}}_e + \widehat{p}_e \right) \end{bmatrix} = 0$$

③ Homogeneous Maxwell's equations

$$\partial_{\widehat{t}} \begin{bmatrix} \widehat{c}\widehat{\mathbf{B}} \\ \widehat{\mathbf{E}} \end{bmatrix} + \widehat{c \nabla \times} \begin{bmatrix} \widehat{\mathbf{E}} \\ -\widehat{c}\widehat{\mathbf{B}} \end{bmatrix} = 0$$

Numerical method: Hyperbolic PDE solver

We used an explicit, finite-volume, shock-capturing numerical method, implemented in Randall LeVeque's CLAWPACK (Conservation LAW PACKage).

Finite Volume method framework in 1 dimension:

- In 1D, our PDE is of the form

$$q_t + f(q)_x = 0.$$

- Finite volume methods for this equation can be written in conservation form:

$$Q_i^{n+1} = Q_i^n - \frac{\Delta t}{\Delta x}(F_{i+1/2}^n - F_{i-1/2}^n),$$

  where Q_i^n represents the cell-average state value (alternately regarded as the state value at the center of the cell), and $F_{i+1/2}^n$ represents the flux rate out of the right cell boundary.
- Need to estimate the fluxes.

Numerical method: Hyperbolic PDE solver

We use an approximate Riemann solver to estimate flux values at each cell interface.

Estimate cell interface fluxes over one time step using an approximate Riemann solver:

- For smooth data our PDE can be written in the form:

$$q_t + f_q \cdot q_x = 0$$

- At each cell interface we approximate with frozen coefficients:

$$q_t + A \cdot q_x = 0,$$

where A represents f_q evaluated at some average (we chose the arithmetic average) of the states in the cells to the left and the right of the interface at the beginning of a time step.

- To compute the interface fluxes evolve a piecewise-linear reconstruction of the initial state using the frozen coefficient PDE over one time step.
- Piecewise-linear reconstruction of initial state:
  - Piecewise-constant = Godunov
  - Connect-the-dots = Lax-Wendroff
  - Slope-limiters = high-resolution
- Slope limiters:
  - Need $eigenstructure$ of flux Jacobian
  - Split the flux jumps into eigenjumps and apply limiters to cap eigenjumps from overshooting neighboring cell values. (We used the MC (Monotonized Central difference) limiter.)

Numerical method: Hyperbolic PDE solver

Formulas to compute numerical fluxes

The fluxes are computed as

$$F_{i-1/2} = F^R_{i-1/2} + \tilde{F}_{i-1/2},$$

where $F^R_{i-1/2}$ is the Riemann flux and $\tilde{F}_{i-1/2}$ is a second-order limited correction flux.

$$\begin{aligned} F^R_{i-1/2} &= \frac{1}{2}\Big(f(Q_{i-1}) + f(Q_i)\Big) \\ &\quad + \frac{1}{2}\Big(\sum_{s_p<0} Z^p_{i-1/2} - \sum_{s_p>0} Z^p_{i-1/2}\Big), \end{aligned}$$

where the "flux waves" $Z^p_{i-1/2}$ are defined by a decomposition of the flux jump in terms of the eigenvalues s^p and corresponding eigenvectors of $\hat{A}_{i-1/2}$, an approximation to $f'(Q_{i-1/2})$:

$$f(Q_i) - f(Q_{i-1}) =: \sum_p Z^p_{i-1/2}).$$

Typically

$$\hat{A}_{i-1/2} = f'\Big(\frac{Q_{i-1} + Q_i}{2}\Big).$$

The correction flux is

$$\tilde{F}_{i-1/2} = \frac{1}{2}\sum_p \mathrm{sgn}(s^p_{i-1/2})\Big(1 - \frac{\Delta t}{\Delta x}|s^p_{i-1/2}|\Big)\,\tilde{Z}^p_{i-1/2}$$

where

$$\tilde{Z}^p_{i-1/2} = \mathrm{vectorLimiter}(Z^p_{i-1/2}, Z^p_{I^p-1/2})$$

where I^p is the upwind index in the p-th eigenvalue:

$$I^p = i - \mathrm{sgn}(s^p)$$

The $\mathrm{vectorLimiter}$ function is typically computed by projecting the second argument onto the first and applying a scalar limiter function:

$$\mathrm{vectorLimiter}(U, V) = \mathrm{scalarLimiter}\Big(1, \frac{U \cdot V}{U \cdot U}\Big)U.$$

Scalar Limiters

How a scalar limiter computes its value:

1. Inputs are a slope (or jump) at an interface and the upwind interface.
2. If the inputs have opposite signs, return 0.
3. Compute a preliminary output.
4. Cap the output by twice the bigger input.

How the preliminary output is computed:

1. **minmod**: the minimum-sized argument (which makes capping unnecessary);
2. **superbee**: the larger of the two arguments;
3. **MC** (monotonized central-difference limiter): the average of the two arguments;
4. **van Leer**: twice the product divided by the sum (which makes capping unnecessary).

Concrete formulas:

$$\text{minmod}(1,\theta) = \begin{cases} 1 & \text{if } 1 \le |\theta| \\ \theta & \text{if } 0 < \theta| \le 1 \\ 0 & \text{if } \theta \le 0 \end{cases},$$

$$\text{superbee}(1,\theta) = \max\big(0, \text{minmod}(1,2\theta), \text{minmod}(2,\theta)\big),$$

$$\text{MC}(1,\theta) = \max\left(0, \min\left(\frac{1+\theta}{2}, 2, 2\theta\right)\right),$$

$$\text{van Leer}(1,\theta) = \begin{cases} 0 & \text{if } \theta \le 0 \\ \frac{2\theta}{1+\theta} & \text{otherwise.} \end{cases}$$

Numerical method: Hyperbolic PDE solver

(Henceforth we drop hats.)

We want to maintain the divergence constraints:

① $\nabla \cdot \mathbf{B} = 0$. Automatically maintained for 1D code.

② $\nabla \cdot \mathbf{E} = \sigma/\epsilon$. We tried:

(a) not enforcing ("cell-centered"), and

(b) Yee scheme (i.e., a staggered grid for E^1).

Computations: Brio-Wu shock problem

We computed solutions to the Brio-Wu 1-dimensional shock problem [BrioWu88].

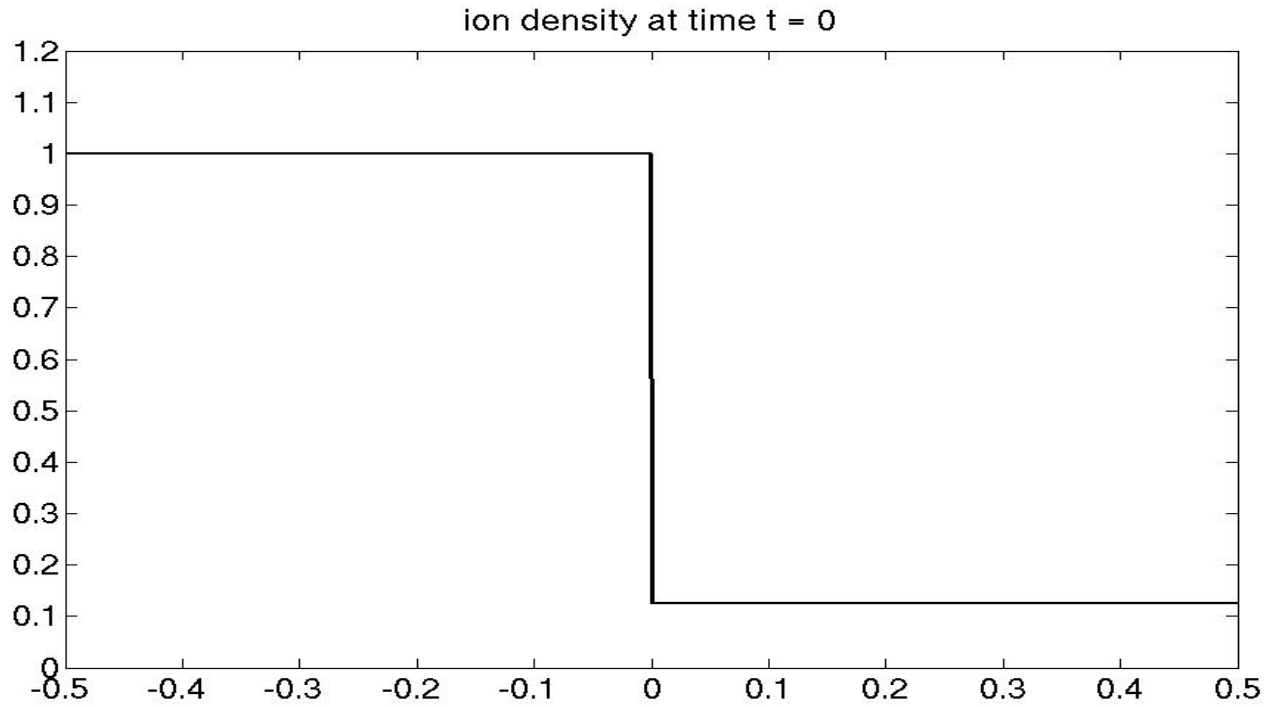

Initial conditions for ion density:
discontinuity at zero, elsewhere constant.

Computations: Brio-Wu shock problem

For **MHD** the Brio-Wu initial conditions to the left and right of zero are:

$$\begin{bmatrix} \rho \\ v^1 \\ v^2 \\ v^3 \\ p \\ B^1 \\ B^2 \\ B^3 \end{bmatrix}_{\text{left}} = \begin{bmatrix} 1.0 \\ 0 \\ 0 \\ 0 \\ 1.0 \\ 0.75 \\ 1.0 \\ 0 \end{bmatrix} \quad \text{and} \quad \begin{bmatrix} \rho \\ v^1 \\ v^2 \\ v^3 \\ p \\ B^1 \\ B^2 \\ B^3 \end{bmatrix}_{\text{right}} = \begin{bmatrix} 0.125 \\ 0 \\ 0 \\ 0 \\ 0.1 \\ 0.75 \\ -1.0 \\ 0 \end{bmatrix}$$

The equivalent **two-fluid** initial conditions are:

$$\begin{bmatrix} \rho_i \\ v_i^1 \\ v_i^2 \\ v_i^3 \\ p_i \\ \rho_e \\ v_e^1 \\ v_e^2 \\ v_e^3 \\ p_e \\ B^1 \\ B^2 \\ B^3 \\ E^1 \\ E^2 \\ E^3 \end{bmatrix}_{\text{left}} = \begin{bmatrix} 1.0 \\ 0 \\ 0 \\ 0 \\ 0.5 \\ 1.0\frac{m_e}{m_i} \\ 0 \\ 0 \\ 0 \\ 0.5 \\ 0.75 \\ 1.0 \\ 0 \\ 0 \\ 0 \\ 0 \end{bmatrix} \quad \text{and} \quad \begin{bmatrix} \rho_i \\ v_i^1 \\ v_i^2 \\ v_i^3 \\ p_i \\ \rho_e \\ v_e^1 \\ v_e^2 \\ v_e^3 \\ p_e \\ B^1 \\ B^2 \\ B^3 \\ E^1 \\ E^2 \\ E^3 \end{bmatrix}_{\text{right}} = \begin{bmatrix} 0.125 \\ 0 \\ 0 \\ 0 \\ 0.05 \\ 0.125\frac{m_e}{m_i} \\ 0 \\ 0 \\ 0 \\ 0.05 \\ 0.75 \\ -1.0 \\ 0 \\ 0 \\ 0 \\ 0 \end{bmatrix}$$

Computations

We plotted ion density at nondimensionalized time $t = 0.1$ for a range of values of the nondimensionalized Larmor radius:

- $r_L = \infty$ (an Euler gas dynamics computation),
- $r_L = 10, 1, 0.1, 0.01, 0.003$ (two-fluid computations), and
- $r_L = 0$ (an ideal MHD computation).

Results:

- As $r_L \longrightarrow 0$, the solution seems to weakly approach the MHD solution.
- For smaller values of r_L computation becomes prohibitively expensive as we need a finer computational grid to prevent negative pressures or densities from crashing the code and to get convergence.
- For intermediate values of r_L, the computational domain needs to be extended the most due to substantial fast-moving oscillations.

Computations (cell-centered), $r_L = 10$

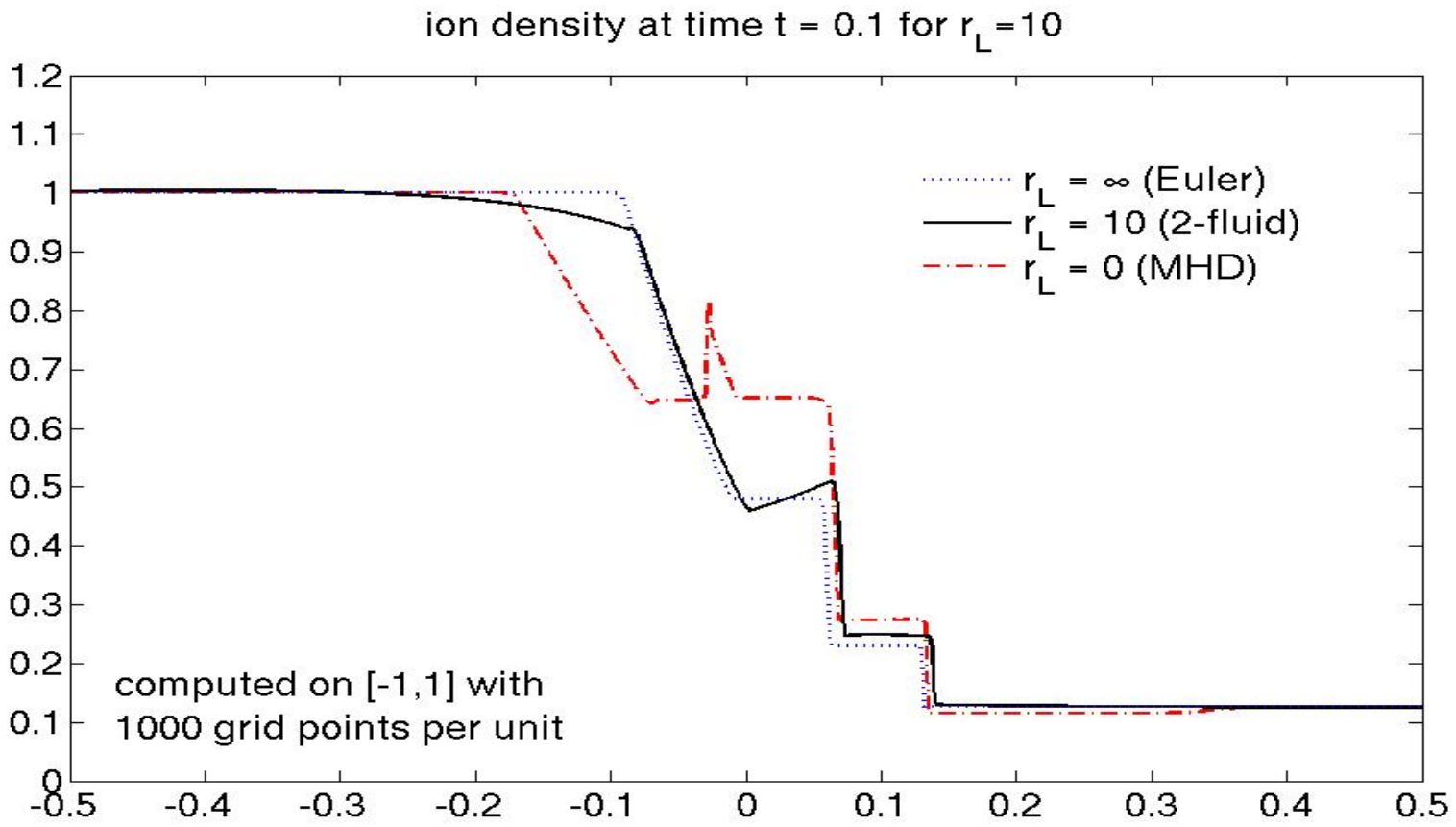

When the Larmor radius is large ($r_L = 10$), the electromagnetic effects are weak and the ions behave like an ideal gas. (At $r_L = 100$, 2-fluid is indistinguishable from Euler.)

Computations (cell-centered), $r_L = 1$

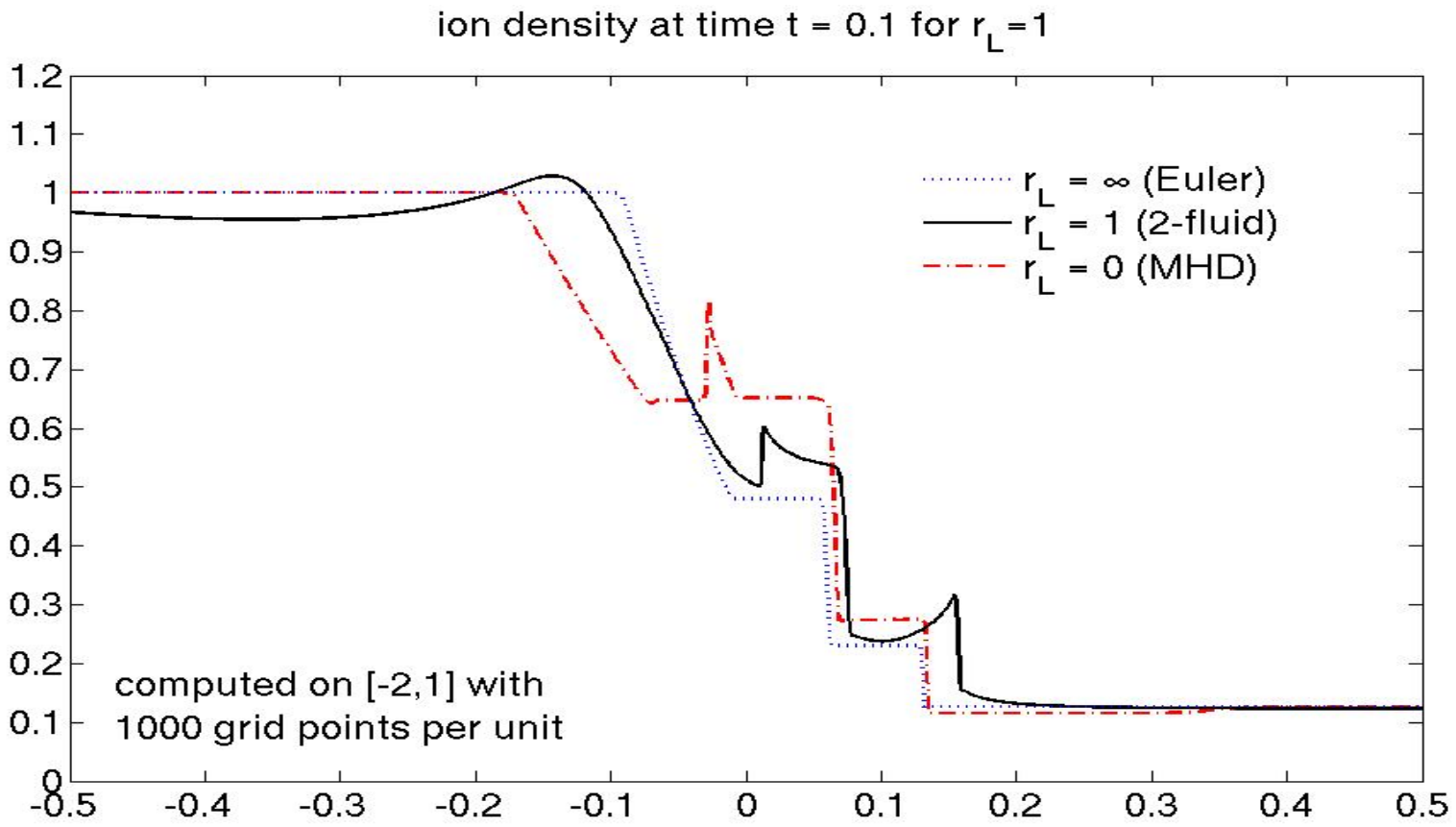

As we decrease the Larmor radius, the solution begins to transition away from gas dynamics (and eventually toward MHD).

Computations (cell-centered), $r_L = 0.1$

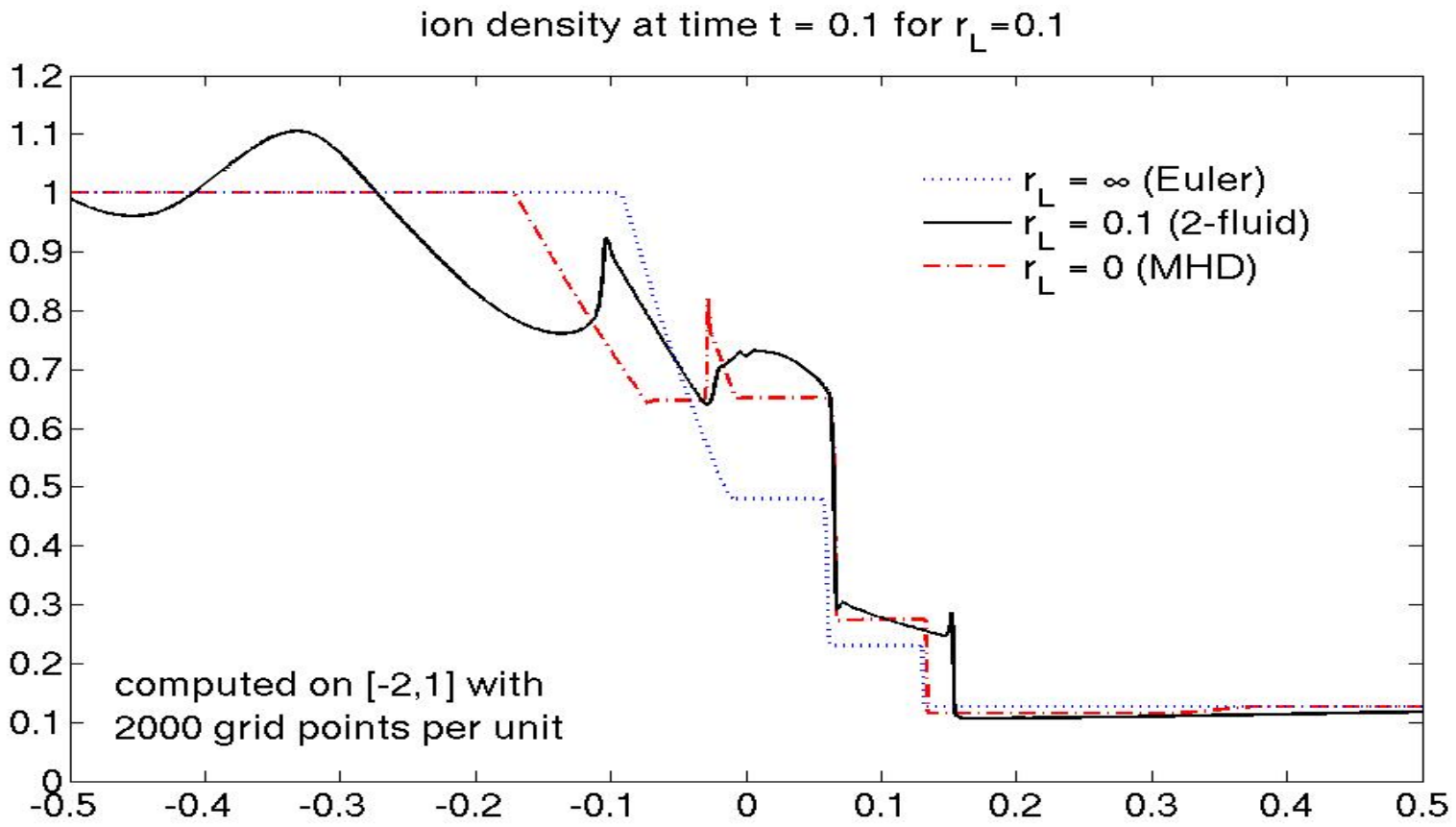

When $t \approx r_L$, the solution is roughly intermediate between Euler and MHD.

Computations (cell-centered), $r_L = 0.01$

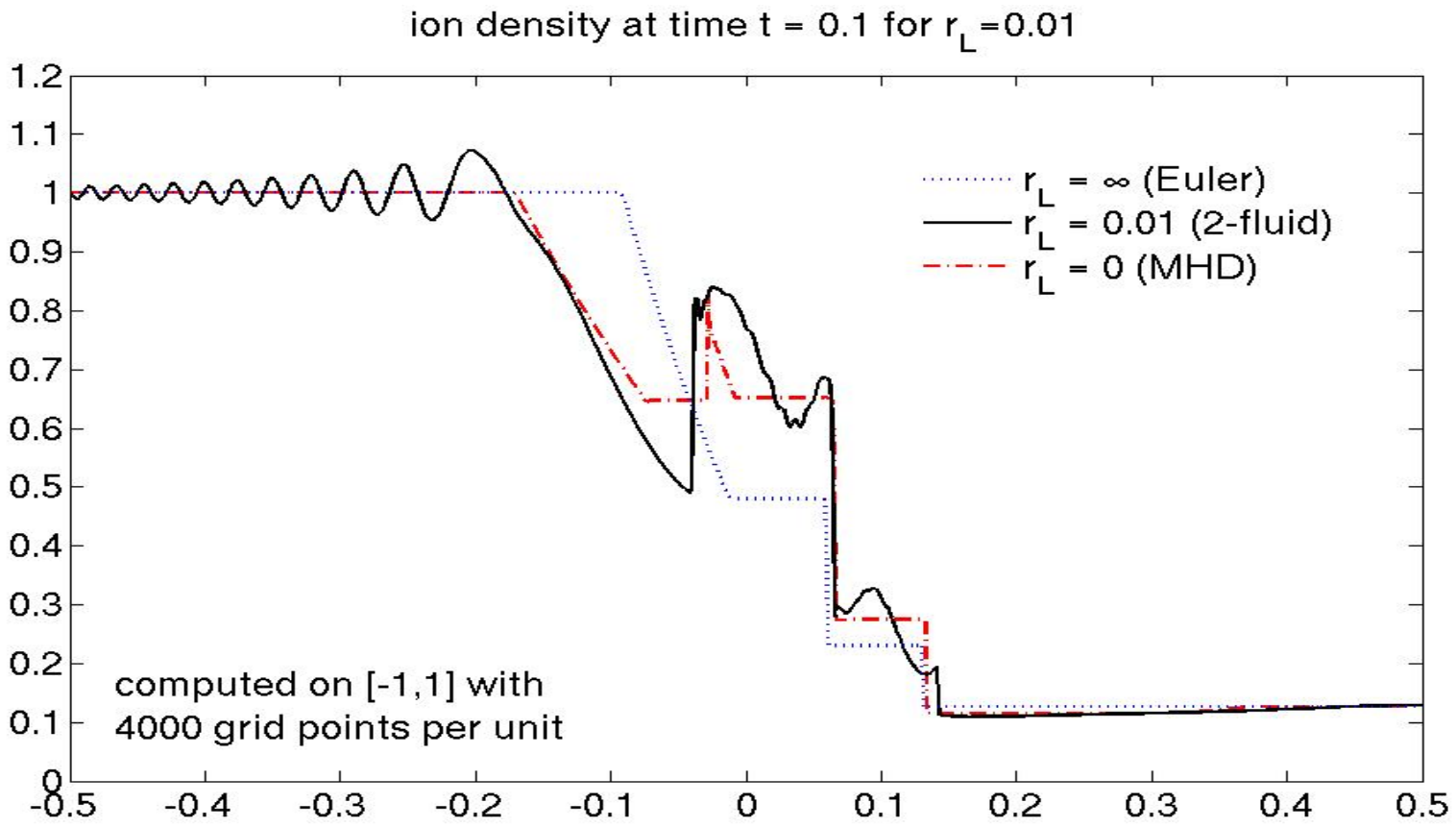

As the Larmor radius becomes even smaller, the frequency of the oscillations increases and the solution begins to weakly approach the MHD solution.

Computations (cell-centered), $r_L = 0.003$

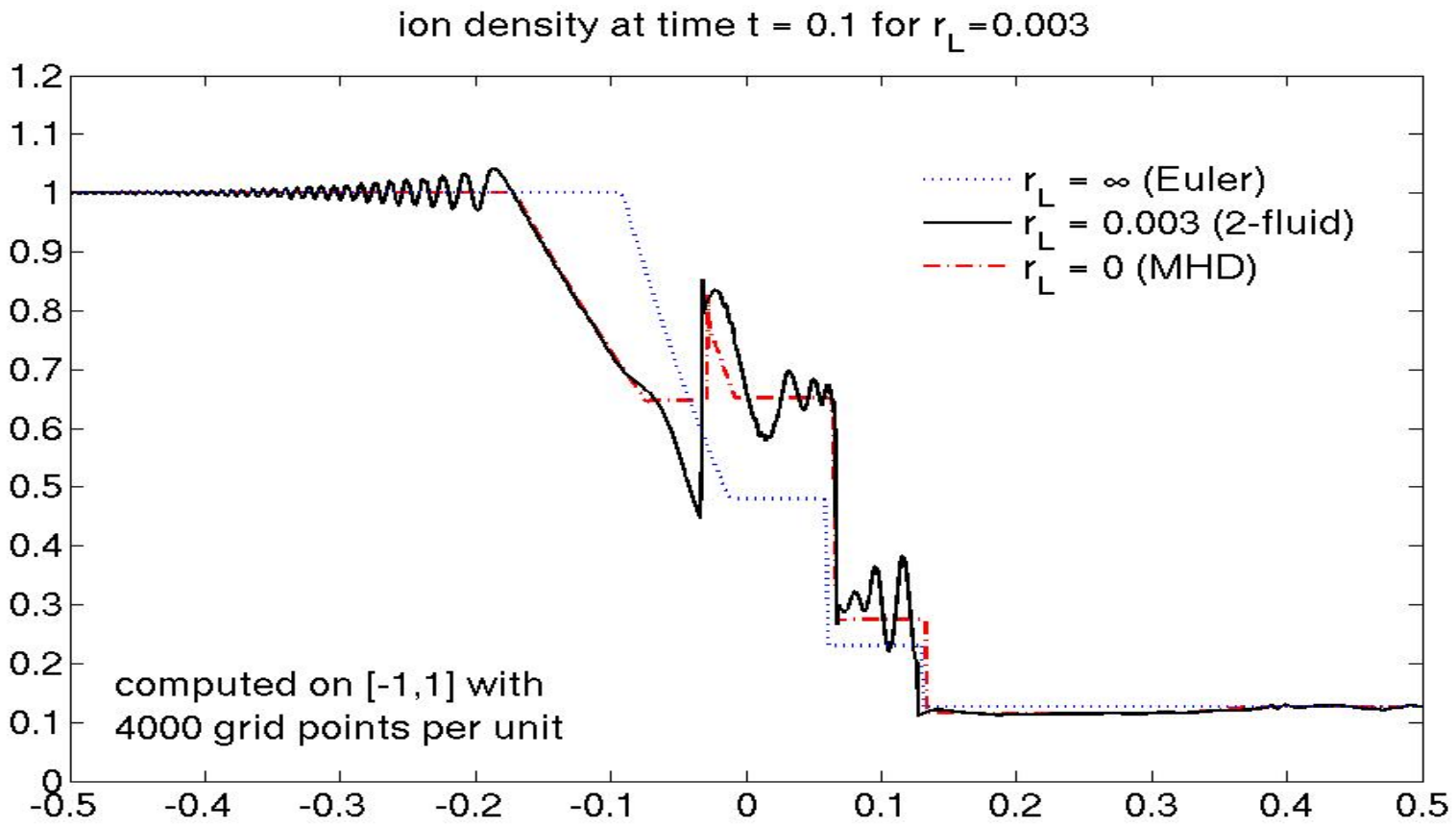

Convergence to MHD is suggested but far from confirmed. Unfortunately, computational expense increases with decreasing Larmor radius.

Computations (cell-centered): **Convergence with mesh-refinement**, $r_L = 0.01$

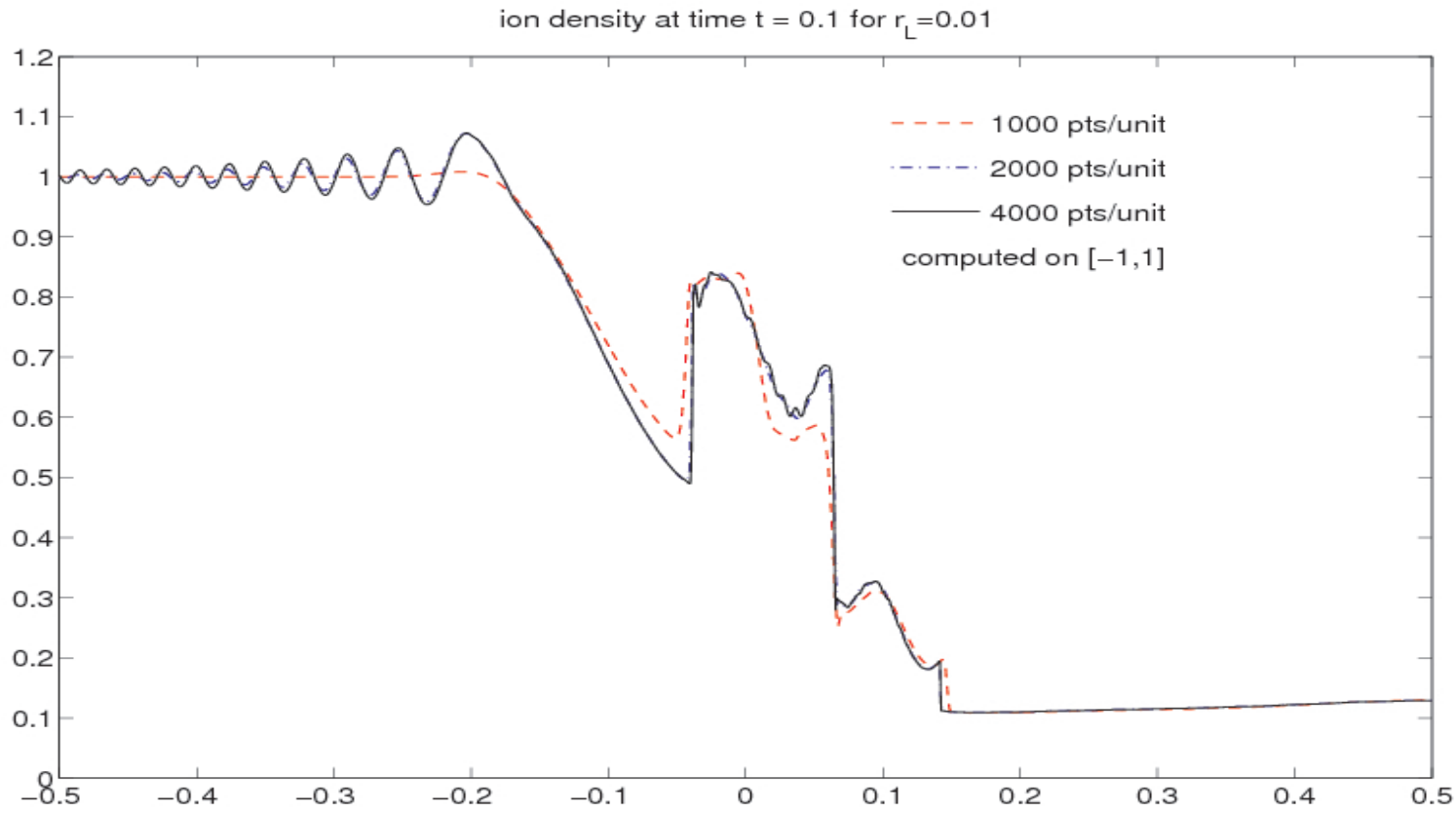

The two solutions with finer resolution (2000 versus 4000 grid points per unit) are almost indistinguishable at the scale of this plot. Notice that the coarse mesh does not resolve the Langmuir oscillations (?) on the left.

Computations (cell-centered): Rate of convergence, $r_L = 0.01$

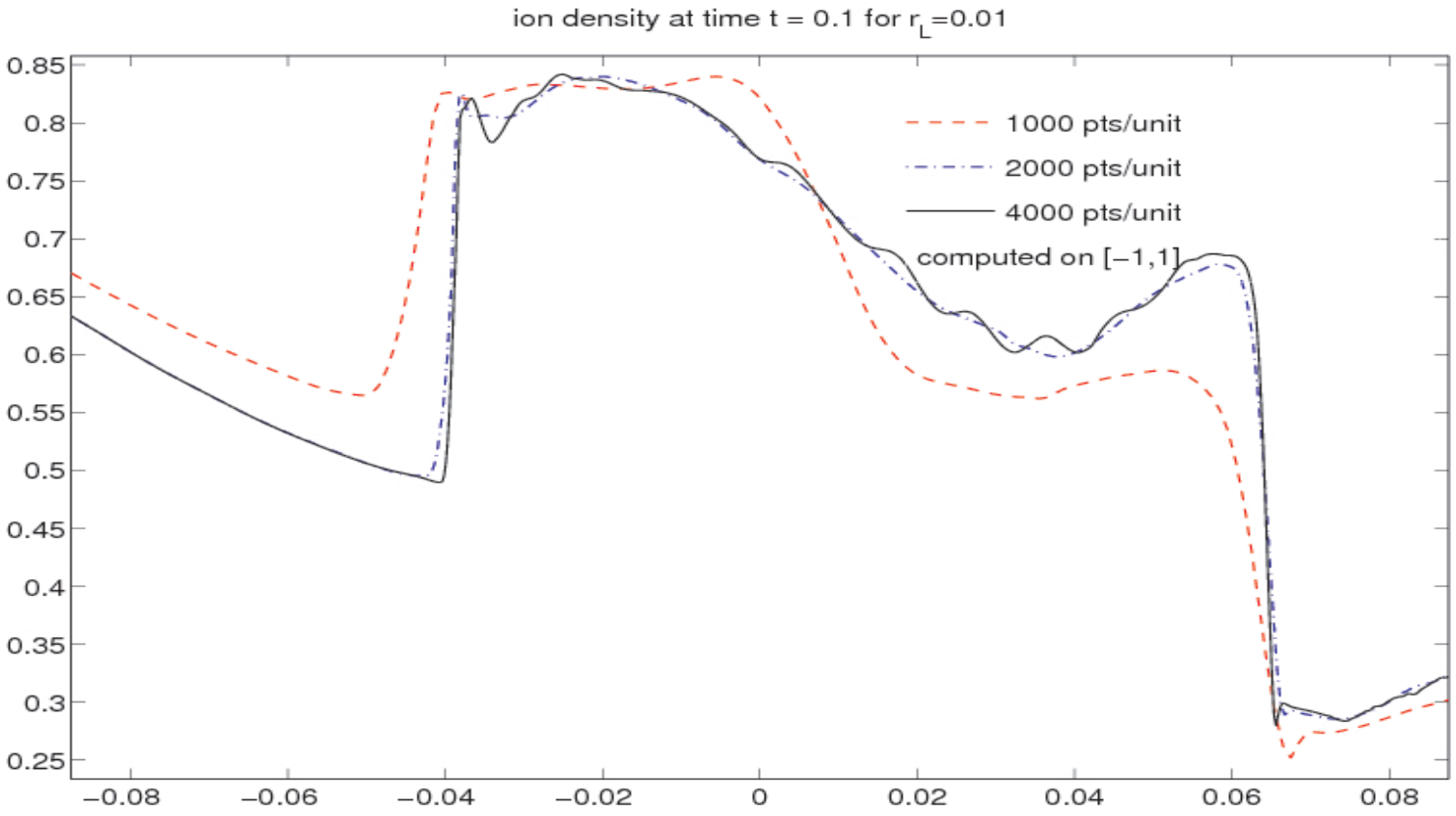

A blow-up of the previous plot showing convergence
near the right end of the slow compound wave of MHD.

Numerical method: Yee scheme

The Yee scheme uses a staggered grid to represent E^1 and maintains the following discretization of the divergence constraint $\nabla \cdot \mathbf{E} = \sigma/\epsilon$:

$$\frac{E^1_{i+1/2} - E^1_{i-1/2}}{\Delta x} = \frac{\sigma_i}{\epsilon}.$$

Yee scheme time step:

① Average the staggered values of E^1 to obtain cell-centered values:

$$E^1_i = \frac{E^1_{i+1/2} + E^1_{i-1/2}}{2}$$

② Use cell-centered solver to update all state values. (We will discard the updated values of E^1_i that this produces.) Retain the computations of flux for the charge densities of the ions and electrons and add them to get a net charge flux:

$$J^{1,n+1/2}_{i+1/2} = J^{1,n+1/2}_{\text{ion},i+1/2} + J^{1,n+1/2}_{\text{electron},i+1/2}$$

③ Update the first component of the electric field by means of:

$$E^{1,n+1}_{i+1/2} = E^{1,n}_{i+1/2} - \frac{\Delta t}{\epsilon} J^{1,n+1/2}_{i+1/2}.$$

Computations with Yee scheme

Results:

- For large Larmor radius the Yee scheme was indistinguishable from the cell-centered scheme.
- For intermediate values of Larmor radius ($r_L = t = 0.1$), the Yee scheme is less accurate for a coarse mesh but more accurate for a fine mesh.
- For small Larmor radius the Yee scheme required a prohibitively small mesh size to prevent negative or vanishing densities.
- Suggested conclusion: Use the cell-centered scheme for a large mesh and switch to the Yee scheme for a sufficiently fine mesh.

Computations, cell-centered, $r_L = 0.1$

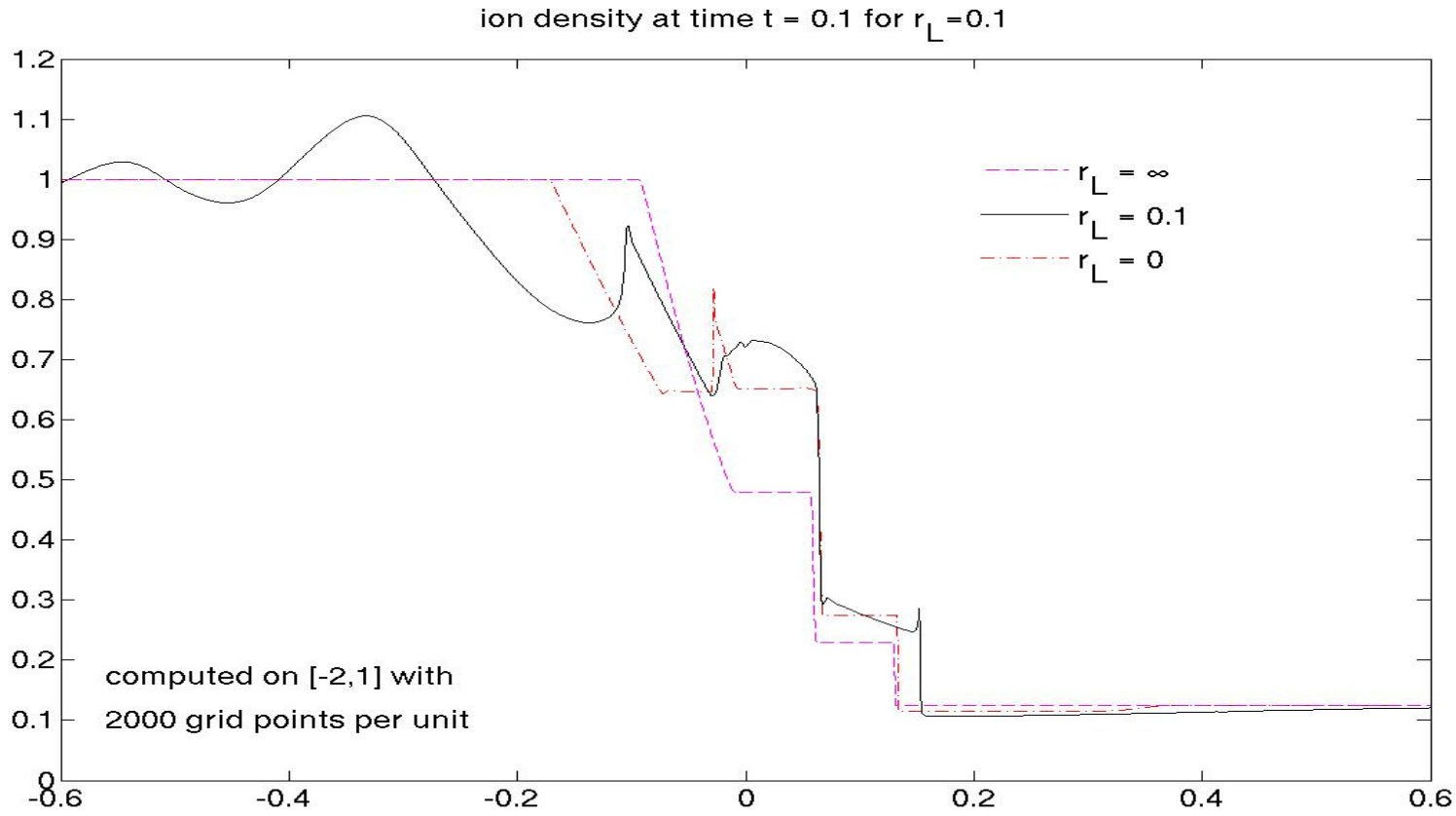

(Cell-centered computation for comparison with Yee scheme.)

Computations: Comparison with Yee scheme, $r_L = 0.1$

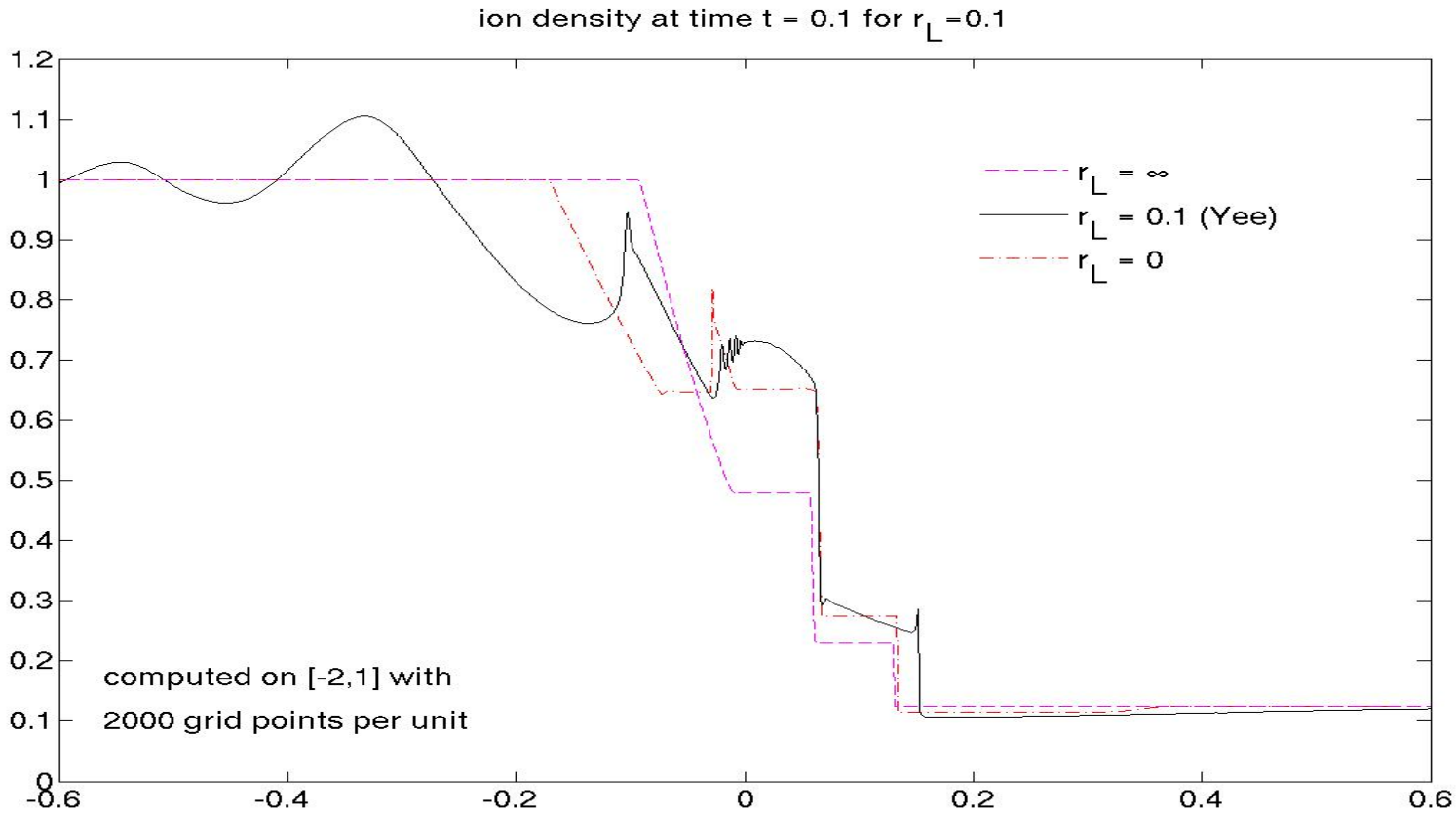

The plot of the Yee scheme is indistinguishable from the unstaggered scheme except in the squiggly area near the right end of the slow compound wave of MHD and the peak in the rarefaction wave of MHD.

Computations: Comparison with Yee scheme, $r_L = 0.1$

Close-up near MHD compound wave.

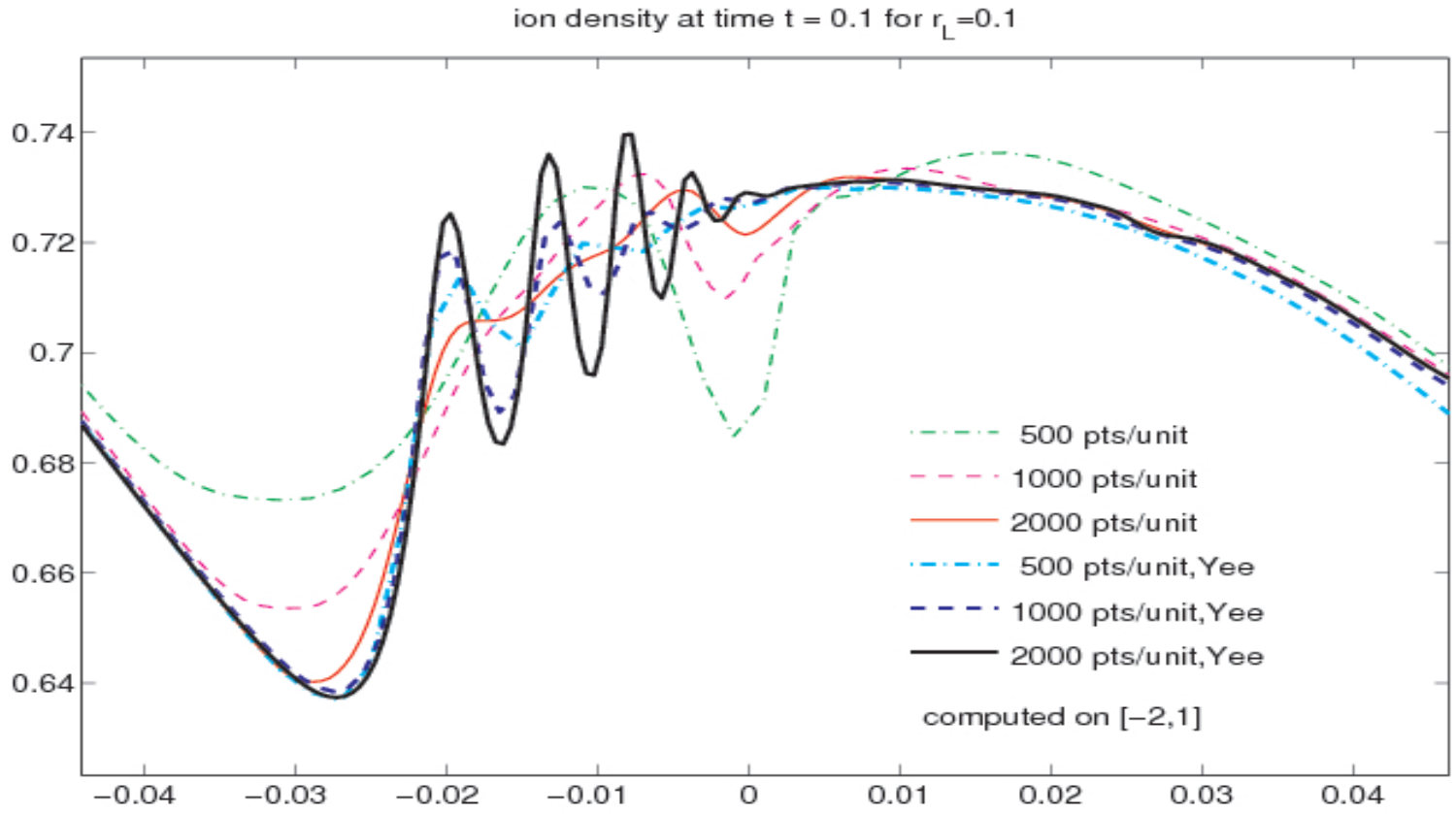

The Yee scheme converges much more rapidly in this region of high oscillation near the right end of the slow compound wave of MHD (compare the highly resolved solution in Fig. 4 of [Hakim06]).

Computations: Comparison with Yee scheme, $r_L = 0.1$

Close-up near MHD fast rarefaction wave.

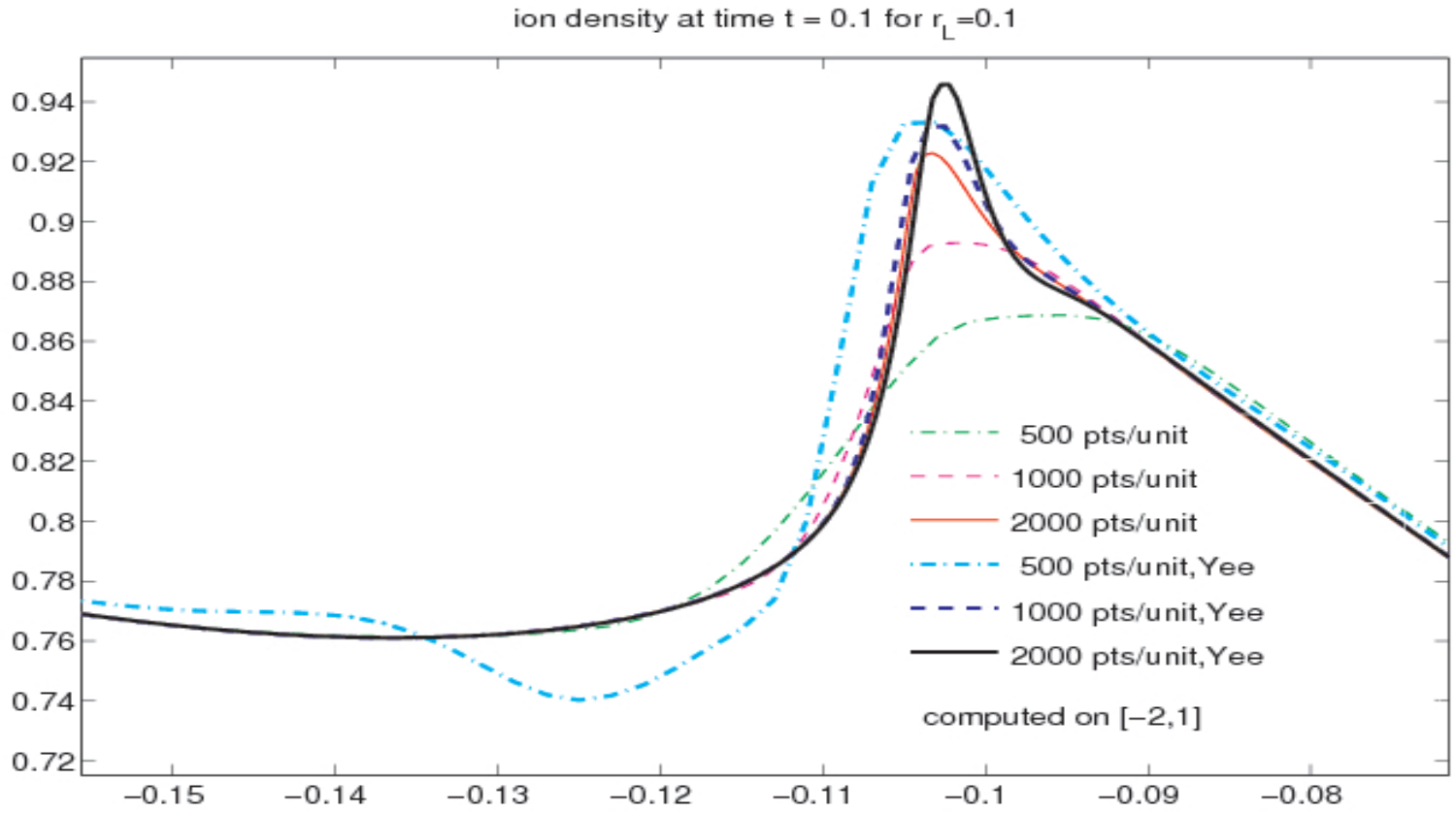

Here at the peak in the MHD rarefaction wave region, the Yee scheme performs more poorly at coarse resolution, but better at fine resolution (compare the highly resolved peak in Fig. 3 of [Hakim06]).

Future work

1. Accelerate 1D solver for Brio-Wu by resolving fast waves and high frequencies only where needed (using techniques such as adaptive mesh refinement and implicit methods), and compare with Hall MHD.
2. Extend solver to 2-dimensions.
3. Obtain a fast solution to a 2D reconnection problem like the Geospace Environmental Modeling (GEM) reconnection challenge problem.
4. Extend solver to special and general relativistic flows.

References

[BrioWu88] M. Brio, C. Wu, *An upwind differencing scheme for the equations of magnetohydrodynamics*, Journal of Computational Physics, 75 (1998) 400-422.

[Shumlak03] U. Shumlak and J. Loverich. *Approximate Riemann solver for the two-fluid plasma model*, Journal of Computational Physics, 187 (2003) 620-638.

[Loverich05] J. Loverich, A. Hakim, U. Shumlak, *A discontinuous Galerkin method for ideal two-fluid plasma equations*, preprint submitted to Journal of Computational Physics, 13 December 2005.

[Hakim06] A. Hakim, J. Loverich, U. Shumlak, *A high resolution wave propagation scheme for ideal two-fluid plasma equations*, Journal of Computational Physics, 219 (2006) 418-442.

[LeVeque02] R. LeVeque, *Finite Volume Methods for Hyperbolic Problems*, Cambridge University Press, 2002.

Acknowledgements

- Sandia National Labs
- Wisconsin Space Grant Consortium
- My advisor, James Rossmanith
- Helpful conversations with Uri Shumlak, Daniel den Hartog, and Carl Sovinec